Floquet Engineering the Quantum Rabi Model in the Ultrastrong Coupling Regime

Kamran Akbari,[1,*] Franco Nori,[2,3,4] and Stephen Hughes[1]

[1] *Department of Physics, Engineering Physics and Astronomy, Queen's University, Kingston, Ontario K7L 3N6, Canada*
[2] *Theoretical Quantum Physics Laboratory, Cluster for Pioneering Research, RIKEN, Wakoshi, Saitama 351-0198, Japan*
[3] *Quantum Computing Center, RiKEN, Wakoshi, Saitama, 351-0198, Japan*
[4] *Physics Department, The University of Michigan, Ann Arbor, Michigan 48109-1040, USA*

(Received 23 July 2024; revised 31 October 2024; accepted 9 January 2025; published 12 February 2025)

We study the quantum Rabi model for a two-level system coupled to a quantized cavity mode under periodic modulation of the cavity-dipole coupling in the ultrastrong coupling regime, leading to rich Floquet states. Exploiting the quantum vacuum, we show how purely mechanical driving can produce real photons, depending on the strength and frequency of the periodic coupling rate. This scheme is promising for the coherent manipulation of hybrid quantum systems and quantum vacuum effects, with potential applications for quantum state engineering, quantum information processing, and the study of non-equilibrium quantum phenomena.

DOI: 10.1103/PhysRevLett.134.063602

Since the early observations with intersubband polaritons [1,2], the ultrastrong coupling (USC) regime of light-matter interactions has emerged as a fascinating and distinctive phenomenon in quantum optics, particularly within the realm of cavity quantum electrodynamics (QED) [3–5]. One intriguing facet of USC is the occupation of virtual excitations (e.g., photons), even in the ground state of the dressed system, which is a consequence of counter-rotating wave effects and breaking U(1) symmetry [3,5,6]. This raises the question of whether it is possible to convert virtual photons into real ones [3,7], which requires input energy, e.g., coherent or incoherent excitation [8,9], to introduce time-dependent characteristics into the system, nonadiabatically [10,11]. Although virtual excitations are not detectable, ideas have been proposed to release them as real excitations [8–10,12–28], e.g., through time modulation of the Rabi frequency [10,14], using flying atoms [28], and exploiting phonon pumping [27,29]. Related ideas have been proposed [30–32] and measured [33,34] in the context of the the dynamical Casimir effect [29,35–37].

In this Letter, we study the nonperturbative "shaking" of a two-level system (TLS), coupled to a single quantized cavity, while in the USC regime. In such a regime, the Jaynes-Cummings model, a cornerstone model under the rotating-wave approximation for explaining weak and strong coupling effects, fails [38–40]. Instead, one must consider the joint atom-cavity dressed states [3,39–41], where even the ground state is an entangled state of photons and matter, which is caused by counter-rotating wave terms in the cavity-TLS interaction Hamiltonian. With such terms, the definitive model in cavity QED is the quantum Rabi model (QRM), which contains nonlinear saturation effects even in vacuum.

However, for driven cavity-QED systems, the QRM can also fail, since strong hybridization of the bare subsystems demands a nonperturbative treatment [39,41]. Often, periodic driving is considered as a weak perturbation that induces transitions between the (predriving) hybrid states [39,42] so that one can utilize a sufficiently low number of the time-independent QRM basis states and employ perturbation theory after the driving. Yet, when the strength of the driving amplitude is also significant, the dressed (joint) light-matter states of the entire system transforms into a Floquet picture, an important theoretical framework for understanding periodically driven systems [43,44]. Apart from its fundamental interest, Floquet theory is a powerful tool for engineering quantum systems [44–55] and reservoirs [50,56,57], and has been used for describing photon-assisted quantum tunneling and transport [44,58–63] and various high-field classical drives including the so-called strong and ultrastrong Floquet drives of bosonic systems [64,65] and carrier-wave Rabi flopping [66–68], where the rotating-wave approximation is relaxed in the (time-dependent) drive term, but the system-level interaction is still of the Jaynes-Cummings model type.

In this Letter, we describe how one can *Floquet engineer the QRM*, in the USC regime, by applying nonperturbative periodic oscillations to the TLS-cavity coupling rate. Moreover, *in USC*, it is essential to uphold the gauge-invariance principle when dealing with truncated matter systems [38–40,69–73]. The hybrid system states evolve nonadiabatically into Floquet quasienergy states, forming new transitions via the newly introduced anticrossings in the Floquet picture. Such periodic modulation can connect to various experimentally accessible regimes, such as the

*Contact author: kamran.akbari@queensu.ca

 © 2025 American Physical Society

dynamical Casimir effect [29,30], surface acoustic waves in semiconductors [74,75], and optomechanical interactions [9], including molecular optomechanics [76–78]. Our significant findings include (i) a double-field (photon plus mechanical oscillation)-assisted splitting of the QRM states due to the renormalization of the time-independent energy states, (ii) production of real photons and TLS excitations from vacuum, and (iii) higher-order nonlinear quantum processes that are effective only in the USC regime.

We begin with the *time-dependent* QRM Hamiltonian

$$\mathcal{H}_{\rm FQR}(t) = \omega_c a^\dagger a + \frac{\omega_a}{2}\{\sigma_z \cos[c(t)] + \sigma_y \sin[c(t)]\}, \quad (1)$$

in the Coulomb gauge [69,73] ($\hbar = 1$), called the Floquet-engineered quantum Rabi (FQR) Hamiltonian, where ω_c (ω_a) is the cavity (TLS) transition frequency, a ($a^\dagger$) is the cavity photon annihilation (creation) operator, σ_i are the TLS Pauli operators, and $c(t) = 2(a + a^\dagger)\eta(t)$. Note this QRM Hamiltonian is quite different from historical (and textbook) QRMs since matter truncation (i.e., a reduced Hilbert space) introduces a nonlocal potential, which causes the minimal coupling replacement to take on a modified form that satisfies the gauge principle [69,73]. This manifests in a gauge-invariant QRM that necessarily contains photon terms to all orders, and it is more convenient (and fundamental) to solve time-dependent interactions in the Coulomb gauge [72,73]. The normalized TLS-cavity coupling rate is $\eta(t) = \eta_0 + \eta_M \sin(\omega_M t)$, where $\eta_0 \equiv g/\omega_c$ (g is the atom-cavity coupling rate), and η_M (ω_M) is the amplitude (frequency) of the time-dependent coupling. The calligraphic notation of the Hamiltonian indicates that the gauge-fixed Hamiltonian is used for the *truncated* matter Hilbert space [39,69,73]. Note that when $\eta(t) \to \eta$, Eq. (1) fully recovers previous time-independent (and gauge-invariant) models [39,40,69].

Figure 1 shows a schematic of our time-dependent QRM. Because of the periodic time-dependent coupling, with period $T = 2\pi/\omega_M$, the Hamiltonian is also periodic: $\mathcal{H}_{\rm FQR}(t) = \mathcal{H}_{\rm FQR}(t + T)$, which can be expanded as a Fourier series $\mathcal{H}_{\rm FQR}(t) = \sum_{m\in\mathbb{Z}} \mathcal{H}_m e^{im\omega_M t}$, with

$$\mathcal{H}_m = \omega_c a^\dagger a \delta_{m0} + \frac{\omega_a}{2}\left\{\frac{\sigma_z - i\sigma_y}{2} e^{i2(a+a^\dagger)\eta_0} + (-1)^m \frac{\sigma_z + i\sigma_y}{2} e^{-i2(a+a^\dagger)\eta_0}\right\} J_m[2(a+a^\dagger)\eta_M], \quad (2)$$

where J_m is the Bessel function of the first kind of order m, and we have used the Anger-Jacobi expansion [79] of Eq. (1). When $\eta_M \to 0$, then $J_0(0) = 1$ and $J_{m\gtrless 0}(0) = 0$, and we recover the time-independent QRM Hamiltonian. In practice, we must also truncate $|m| \leq m_{\rm max}$. Note also that $\mathcal{H}_m$ separates into a time-independent part for $m = 0$ (including a shift due to $\eta_M \neq 0$), and a time-dependent interaction (for $m \neq 0$). Thus, while η_M is related to the time-dependent light-matter interaction, there is a static contribution from the J_0 term. While Eq. (1) accounts for the static dressing via photon-matter interactions, Eq. (2) *dresses* the entire cavity-QED system with periodic mechanical oscillations. Similar expressions are widely considered for single quantum systems, including field-driven TLSs [80].

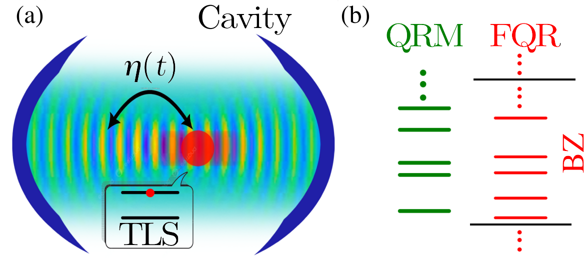

FIG. 1. (a) Schematic of a TLS with a mechanical vibration inside a cavity with a dominant single mode. (b) Without the mechanical vibration, the system is identified by the usual (time-independent) QRM Hamiltonian with N_j dressed states (left); after the periodic vibration is turned on, the FQR quasienergies and states govern the system (right) transitions, with N_j of them in one Brillouin zone (BZ).

For numerical calculations, the time-independent $\mathcal{H}_0$ is first diagonalized with the eigenbasis $\{E_j, |j\rangle\}_{j=0}^{N_j-1}$, where N_j is the number of truncated ac-shifted quantum-Rabi-dressed states, obtained from $\mathcal{H}_0|j\rangle = E_j|j\rangle$, which satisfies the conditions $\langle j|j'\rangle = \delta_{jj'}$ and $\sum_{jj'} |j\rangle\langle j'| = \mathbf{1}$; here, E_j ($|j\rangle$) are shifted QRM eigenenergies (eigenstates) renormalized by the presence of the nonzero $\eta_{\rm M}$, since the time-independent portion of the Hamiltonian is $\mathcal{H}_0$, and not $\mathcal{H}_{\rm QRM} = \omega_c a^\dagger a + (\omega_a/2)\{\sigma_z \cos[c(0)] + \sigma_y \sin[c(0)]\}$. This also ensures that we use the correct static states of the joint light-matter system in the presence of driving.

Solving the time-dependent Schrödinger equation, $i\partial_t|\psi(t)\rangle = \mathcal{H}_{\rm FQR}(t)|\psi(t)\rangle$, yields $|\psi_\alpha(t)\rangle = e^{-i\varepsilon_\alpha t}|\alpha(t)\rangle$, where ε_α is the Floquet quasienergy [81], and the Floquet mode $|\alpha(t)\rangle$ is T-periodic [43,82]. The Floquet states, $\{|\psi_\alpha(t)\rangle\}$, form a complete basis for any value of t, thus $|\psi(t)\rangle = \sum_\alpha c_\alpha |\psi_\alpha(t)\rangle$, where $c_\alpha = \langle\alpha|\psi(0)\rangle$, with $|\alpha\rangle \equiv |\alpha(0)\rangle$. Transition resonances occur at differences between Floquet energies [83]. To compute the Floquet modes, we use a Fourier series expansion of $|\alpha(t)\rangle = \sum_{l\in\mathbb{Z}} e^{il\omega_M t}|\alpha_l\rangle$, where the Fourier coefficient states $|\alpha_l\rangle$ are *Floquet sidebands*. There are N_j quasienergies confined within a $[-\omega_M/2, \omega_M/2]$ energy range (first BZ), associated with N_j linearly independent Floquet modes [84].

In Fig. 2(a), we plot the eigenenergies versus η_0, from the *time-independent* part of the total Hamiltonian in Eq. (1), i.e., using $\mathcal{H}_0$ from Eq. (2), for a fixed value of $\eta_M = 0.5$ (solid curves), and show how these compare with the standard QRM (dashed curves). This demonstrates how

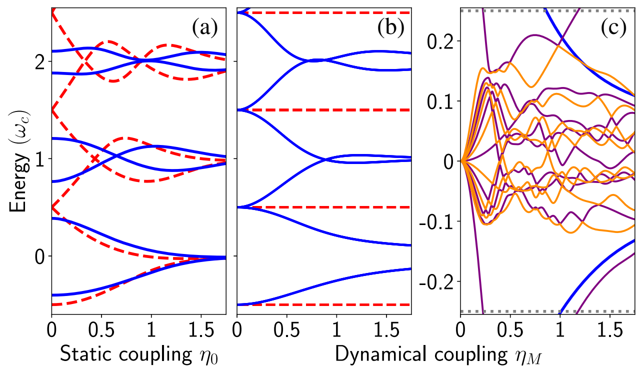

FIG. 2. (a) Eigenenergies obtained from Eq. (2) for $m = 0$ with $\eta_M = 0$ (QRM, dashed curved), and for $\eta_M = 0.5$ (solid lines), versus η_0. (b) Eigenenergies obtained from Eq. (2) again for $m = 0$ (i.e., static part), but now as a function of finite η_M (solid lines), with $\eta_0 = 0$, as well as the QRM eigenenergies (dashed lines). (c) Floquet quasienergies in the first BZ for $\eta_0 = 0$, versus η_M. Thin solid (with every other purple and dark orange color to show anticrossings) lines represent different Floquet quasienergies. Thicker lower and upper blue curves are the first two shifted eigenenergies from panel (b). The parameters used are $\omega_M = 0.5\omega_c$, $\omega_a = \omega_c$, $N_j = 16$, $m_{\max} = l_{\max} = 20$ (see text).

time modulation introduces an effective static (dc) dressing of the QRM eigenenergies. Also, we note from the form of the solid curves that the levels are initially split, i.e., at $\eta_0 = 0$, with more significant splittings for higher energy levels. As η_0 increases, we then enter a regime of *double dressing*, emphasizing that the (nonperturbatively) dressed light-matter QRM states undergo mechanical dressing, nonperturbatively, again.

In Fig. 2(b), we show the eigenenergies of the *time-independent* part of the total Hamiltonian in Eq. (1), characterized by $\mathcal{H}_0$ in the expansion terms in Eq. (2), in comparison with the eigenenergies of the QRM, versus η_M, for $\eta_0 = 0$. There is a renormalization of the eigenenergies, and then a modified anticrossing of the time-independent (static) eigenenergies. The renormalization of the QRM in the Coulomb gauge is a result of the correct gauge-invariant model treated nonperturbatively with the mechanical dressing and is substantially different from the usual dc/ac Stark shift. Note that as one transitions toward USC (i.e., $\eta_M > 0.1$), the shifts (which are independent of ω_M) are amplified until they form new anticrossing regions. When $\eta_0 = \eta_M = 0$, there is no QRM dressing and no hybridization between the light and matter states [dashed lines in panel 2(b)]. By increasing the static coupling $\eta_0 > 0$ when $\eta_M = 0$ [dashed lines in panel 2(a)], the light-matter hybridization begins, where the states are closer to each other, e.g., the first excited state is pushed closer to the ground state, and the second and third excited states move closer. As η_M increases, this boosts the hybridization in such a way that they form new anticrossings at certain field strengths, which depends on the state levels.

We next transform the problem to the Floquet picture. In Fig. 2(c), the Floquet quasienergies within the first BZ are shown for the QRM truncated with 16 states, so that at each value of the drive's parameters, there exist (nominally) 16 quasienergy states within one BZ. Although the original initial-time states are the QRM states, the Floquet states are built upon the renormalized states from the dynamical coupling. The dc component alters the transition strength between dressed states and induces intermixing of the QRM states. Because of the greater number of strongly coupled nearby states in the dc-renormalized Hamiltonian, nonlinear optical effects can occur at a much lower dynamical coupling strength than they would in the absence of the dc coupling, strongly enhancing the transition probabilities [94–96]. This manifests in a rich Floquet quasienergy diagram, shown in Fig. 2(c), which yields a large number of anticrossings [95–100]. These quasienergies are continuous functions of the drive amplitude that shows avoided crossings if there are no symmetries that allow crossings.

In USC, transitions are not between the system bare states (with fixed numbers of photons and atomic excitations), but between the *dressed states of the composite system* [18,28,39,73]. Thus, one must uses the correct dressed operators [39,41] $s^{\Lambda+} = \sum_{j,k>j} S^{\Lambda}_{jk}|j\rangle\langle k|$, where $s^{\Lambda-} = [s^{\Lambda+}]^{\dagger}$, with $\Lambda = \{\mathrm{cav}, \mathrm{TLS}\}$ and $S^{\Lambda}_{jk} \equiv \langle j|S^{\Lambda}|k\rangle$ is the matrix element of the system operator in the Schrödinger picture. Specifically, we use $S^{\mathrm{cav}} = a(1+\mathrm{i})/\sqrt{2} + \mathrm{H.c.}$ [101], and $S^{\mathrm{TLS}} = \sigma_x$.

Next, we study how one can produce real photons. Initially, the system is in the dressed ground state $|j = 0\rangle$. The number of real photons or TLS excitations are defined from [28,39,41] $N_{\Lambda}(t) = \langle\psi(t)|s^{\Lambda-}s^{\Lambda+}|\psi(t)\rangle$. In contrast, the virtual photon number in the ground state of the time-independent light-matter Hamiltonian is [6,28] $\langle 0|a^{\dagger}a|0\rangle_{\mathrm{QR}}$, which is nonzero in vacuum USC [3,6]. An observable, $\langle\psi(t)|O|\psi(t)\rangle$, is not necessarily time periodic due to the presence of off-diagonal terms in the Floquet eigenbasis [102], $e^{\mathrm{i}(\varepsilon_\alpha-\varepsilon_\beta)(t-t_0)}\langle\alpha(t)|O|\beta(t)\rangle$, for $\alpha \neq \beta$ (see Fig. S3 in [84]). However, in real open systems, the off-diagonal terms are suppressed, and the time evolution of observables often becomes periodic. We thus add a damping rate, γ, to the nondiagonal terms, which are damped out in the long time limit [6,96,102]. Subsequently, we derive the expectation values

$$N_{\Lambda}(t) = \sum_{\alpha\beta} c^{*}_{\alpha} c_{\beta} e^{\mathrm{i}(\varepsilon_\alpha-\varepsilon_\beta)t-\gamma t(1-\delta_{\alpha\beta})}\langle\alpha(t)|s^{\Lambda-}s^{\Lambda+}|\beta(t)\rangle \quad (3)$$

and obtain the steady-state solution $N_{\Lambda}(t > t_{\mathrm{ss}}) = \sum_{\alpha} |c_{\alpha}|^2\langle\alpha(t)|s^{\Lambda-}s^{\Lambda+}|\alpha(t)\rangle$. The mean real excitation number is $\bar{N}_{\Lambda} = (1/T)\int_{t_{\mathrm{ss}}}^{t_{\mathrm{ss}}+T} dt\, N_{\Lambda}(t)$, where T is sufficiently long to yield a steady-state average.

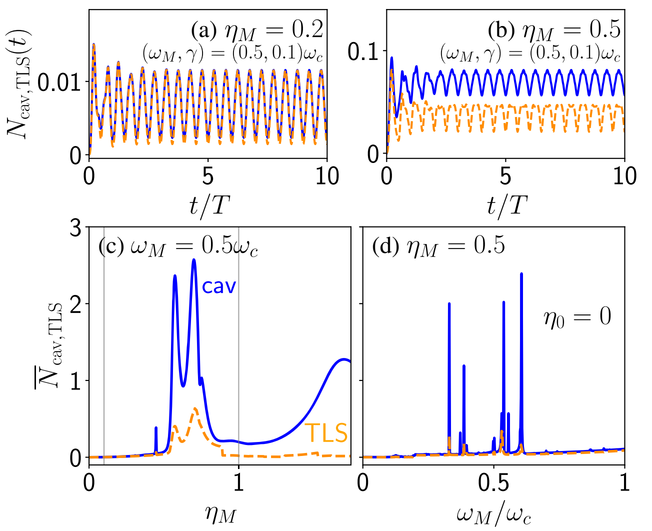

FIG. 3. An example of the time-dependent real excitations, $N_{\mathrm{cav}}(t)$ (real photons, solid blue line) and $N_{\mathrm{TLS}}(t)$ (real TLS excitation, dashed orange line), given by Eq. (3), is shown for (a) $\eta_M = 0.2$ and (b) $\eta_M = 0.5$, with $\gamma = 0.1\omega_c$. Also, depicted are the *mean excitation numbers* that are the temporal average of the cavity excitation number, $\bar{N}_{\mathrm{cav}}$ (solid blue line) and the TLS excitation number, $\bar{N}_{\mathrm{TLS}}$ (dashed orange line), versus the amplitude (c) and frequency (d) of the dynamical coupling. The parameters used are $\eta_0 = 0$, $\omega_a = \omega_c$ and $m_{\mathrm{max}} = l_{\mathrm{max}} = 20$. The gray vertical lines at $\eta_M = 0.1$ and $\eta_M = 1$ in panel (c) span the USC to the deep-USC regime.

In Fig. 3, we show $N_{\mathrm{cav,TLS}}(t)$, with zero static coupling, $\eta_0 = 0$, for different dynamical values of (a),(b) $\eta_M = 0.2$, 0.5, using $\omega_M = 0.5\omega_c = 0.5\omega_a$. The results are periodic after a sufficiently long time, depending on the strength and frequency of dynamical coupling. For increasing coupling, the periodic modulation causes a significant production of real photons (solid curves) and TLS excitation (dashed curves). This scenario requires $\eta_M \neq 0$ and the USC regime. Note that the populations of the cavity are different to the TLS for increasing η_M.

In Fig. 3(c), we plot the average real excitation numbers ($\bar{N}_{\mathrm{cav,TLS}}$), versus η_M, with $\omega_M = 0.5\omega_c$ and $\eta_0 = 0$. Finite η_0 simulations are discussed in the Supplemental Material [84]. We also observe that the onset of USC (or switching on and off within the USC, i.e., the joint effect of the static and dynamical couplings) coincides with the starting point of turning virtual photons into real ones, where there exists the discrepancy between real and virtual photons [28], i.e., $\eta_M \geq 0.1$ since $\eta_0 = 0$. In Fig. 3(d), we show $\bar{N}_{\mathrm{cav,TLS}}$ versus ω_M, with a fixed $\eta_M = 0.5$, for the cavity (solid blue) and the TLS (dashed orange) excitations. From panel 3(d), we generally understand that because the switching on and off process is already in the USC, namely, because $\eta_M > 0.1$, the starting point of turning virtual photons into real ones begins as soon as $\omega_M > 0$, where we also observe a difference between the real photons and the TLS excitations.

The results in Figs. 3(c) and 3(d) are obtained for 16 QRM states and $m_{\mathrm{max}} = l_{\mathrm{max}} = 20$. Adding more truncated QRM states may modify some of the frequency and coupling peaks, and add additional sharper peaks, but in practice these will be broadened with dissipation. Importantly, our main predictions are not qualitatively affected by a further increase in basis size. The general intuitive behavior of the spectral shape is that as the amplitude and frequency of the dynamical coupling increase within the USC range, the number of real photons and TLS excitations become larger because of the enhanced nonlinearity of the quantum processes. However, the emergence of the peaks related to the higher-order quantum processes modifies the linearity of the number spectrum and creates more interesting features. These (doubly nonlinear) peaks are due to nonperturbative double dressing of the quantum system, once by the quantum field of the cavity and then by the classical mechanical vibration field.

The peak and valley structures seen in Figs. 3(c) and 3(d) are connected to the anticrossings of the Floquet quasienergy spectrum. Moreover, higher multioscillation peaks are narrower than lower-oscillation peaks and they form earlier (smaller values) in amplitude and frequency of the drive. This general effect of an increasing spectral width of an absorption line with the increase in the steady source intensity is similar to the power broadening effect in atomic absorption spectra [103].

To highlight some general features, the main cavity double peak and valley structure in Fig. 3(c) is formed by the combination of a 3-ω_M resonance transition ($j = 0 \to 3$) and a 15-ω_M resonance transition ($j = 0 \to 15$). In the first BZ of the quasienergy diagram [Figs. 1(c) and S2(b)], the most effective corresponding anticrossing (which is also quite wide due to nonlinear power broadening) at the same points between the two Floquet sidebands $|\alpha_l = 12_l\rangle$ and $|\alpha_l = 14_l\rangle$ (see Fig. S2 of [84]). Moreover, the very wide power-broadened peak at the far right of the panel, in the deep-USC regime, is a 4-ω_M peak due to the transition from the ground state to the fourth excited state. Because of the enhancement of nonlinear higher-order quantum processes in USC, the peaks are stronger, narrower, and less power-broadened in comparison to those in other regions such as the deep USC.

Note that the creation of each individual peak and also the interplay between the different order transitions and peaks are crucial in the overall construction and understanding of the population spectra. These manifest in the constructive and destructive nonlinear interaction of peaks with various widths and strengths, which can cause a sudden dip or rise, and nonlinear features [96,104–107] such as power broadening, dynamical Stark shift, Autler-Townes multiplet splitting, electromagnetically induced transparency, and hole burning. For example, the drop at $\eta_M \sim 0.9$ of the TLS graph in Fig. 3(c) is caused by the destructive interference of transitions. Spectral modifications arise due to Stark splitting of the driven system energy levels where the decaying system process (atomic down transition in the dressed states) from the two dressed states interferes destructively to create a Fano-type dark line in a single Lorentzian peak [94–96,105]. Similar explanations are applicable for other resonant peaks in the same graph as well as those in Fig. 3(d), which shows the role of increasing ω_M for fixed $\eta_M = 0.5$ [84].

We note that in the USC regime, due to the presence of the counter-rotating waves, the Hamiltonian is not number-conserving. As such, the dressed QRM states provide excitations with different populations of matter and photonic fields, even the ground state. Thus, we already have nonlinearity from this first light-matter dressing, and any possible transition already provides a nonlinear process without even having a strong drive, in contrast to the linear one-photon transitions of weak or strong coupling regimes of cavity QED. However, the *second dressing*, which is the mechanical dressing as a result of the nonperturbative coupling modulating drive, then causes a *second nonlinearity*. Thus, additional higher-order processes are provided with the capability of exchanging multiple mechanical quanta at a time (we have an exponential time term with $\pm l\omega_M$ in the system dynamics), causing rich spectral features in Figs. 3(c) and 3(d).

Lastly, we comment on the role of the $\eta(t)$ waveform. With a pure harmonic $\eta(t)$ waveform, one can drive frequencies comparable to a few fractions of the photon frequency, as known in the context of the dynamical Casimir effect. Generally, one understands that the production of virtual to real excitations must be done nonadiabatically, which means a sudden switch on and switch off of an interaction. Hence, it is expected that nonsmooth waveforms, such as a periodic array of sudden ramps (sawtooth) or top-hat functions, are comparatively highly productive [108]. These forms are also discussed in the Supplementary Material [84].

In summary, we have introduced a Floquet engineered QRM, where a cavity-QED system in the USC regime is subject to a time-periodic cavity-atom coupling rate. By using a suitable gauge-invariant model Hamiltonian, we show how one can generate real excitations out of vacuum through a mechanical oscillation of the location of the atom (or the cavity). Beyond fundamental aspects of nonperturbative vacuum field engineering, our Letter can potentially motivate investigations toward rich quantum light production out of vacuum, as well as the coherent manipulation of quantum systems and nonequilibrium quantum optical effects such as phase transitions, entanglement, and information processing by Floquet engineering the multiphoton correlation functions.

Acknowledgments—This work was supported by the Natural Sciences and Engineering Research Council of Canada (NSERC), the National Research Council of Canada (NRC), the Canadian Foundation for Innovation (CFI), and Queen's University, Canada. S. H. acknowledges the Japan Society for the Promotion of Science (JSPS) for funding support through an Invitational Fellowship. F. N. is supported in part by the Japan Science and Technology Agency (JST) [via the CREST Quantum Frontiers program Grant No. JPMJCR24I2, the Quantum Leap Flagship Program (Q-LEAP), and the Moonshot R&D Grant No. JPMJMS2061], and the Office of Naval Research (ONR) Global (via Grant No. N62909-23-1-2074).

[1] A. A. Anappara, S. De Liberato, A. Tredicucci, C. Ciuti, G. Biasiol, L. Sorba, and F. Beltram, Signatures of the ultrastrong light-matter coupling regime, Phys. Rev. B **79**, 201303(R) (2009).

[2] B. Zaks, D. Stehr, T.-A. Truong, P. M. Petroff, S. Hughes, and M. S. Sherwin, THz-driven quantum wells: Coulomb interactions and stark shifts in the ultrastrong coupling regime, New J. Phys. **13**, 083009 (2011).

[3] A. Frisk Kockum, A. Miranowicz, S. De Liberato, S. Savasta, and F. Nori, Ultrastrong coupling between light and matter, Nat. Rev. Phys. **1**, 19 (2019).

[4] P. Forn-Díaz, L. Lamata, E. Rico, J. Kono, and E. Solano, Ultrastrong coupling regimes of light-matter interaction, Rev. Mod. Phys. **91**, 025005 (2019).

[5] W. Qin, A. F. Kockum, C. S. Muñoz, A. Miranowicz, and F. Nori, Quantum amplification and simulation of strong and ultrastrong coupling of light and matter, Phys. Reports **1078**, 1 (2024).

[6] S. De Liberato, Virtual photons in the ground state of a dissipative system, Nat. Commun. **8**, 1465 (2017).

[7] A. F. Kockum, A. Miranowicz, V. Macrì, S. Savasta, and F. Nori, Deterministic quantum nonlinear optics with single atoms and virtual photons, Phys. Rev. A **95**, 063849 (2017).

[8] T. Werlang, A. V. Dodonov, E. I. Duzzioni, and C. J. Villas-Bôas, Rabi model beyond the rotating-wave approximation: Generation of photons from vacuum through decoherence, Phys. Rev. A **78**, 053805 (2008).

[9] M. Cirio, K. Debnath, N. Lambert, and F. Nori, Amplified optomechanical transduction of virtual radiation pressure, Phys. Rev. Lett. **119**, 053601 (2017).

[10] C. Ciuti, G. Bastard, and I. Carusotto, Quantum vacuum properties of the intersubband cavity polariton field, Phys. Rev. B **72**, 115303 (2005).

[11] P. D. Nation, J. R. Johansson, M. P. Blencowe, and F. Nori, Colloquium: Stimulating uncertainty: Amplifying the quantum vacuum with superconducting circuits, Rev. Mod. Phys. **84**, 1 (2012).

[12] J. Lolli, A. Baksic, D. Nagy, V. E. Manucharyan, and C. Ciuti, Ancillary qubit spectroscopy of vacua in cavity and circuit quantum electrodynamics, Phys. Rev. Lett. **114**, 183601 (2015).

[13] A. Ridolfo, J. Rajendran, L. Giannelli, E. Paladino, and G. Falci, Probing ultrastrong light-matter coupling in open quantum systems, Eur. Phys. J. Special Topics **230**, 941 (2021).

[14] S. De Liberato, C. Ciuti, and I. Carusotto, Quantum vacuum radiation spectra from a semiconductor microcavity with a time-modulated vacuum Rabi frequency, Phys. Rev. Lett. **98**, 103602 (2007).

[15] K. Takashima, N. Hatakenaka, S. Kurihara, and A. Zeilinger, Nonstationary boundary effect for a quantum flux in superconducting nanocircuits, J. Phys. A **41**, 164036 (2008).

[16] A. V. Dodonov, L. C. Celeri, F. Pascoal, M. D. Lukin, and S. F. Yelin, Photon generation from vacuum in nonstationary circuit QED, arXiv:0806.4035.

[17] A. V. Dodonov, Photon creation from vacuum, and interactions engineering in nonstationary circuit QED, J. Phys. Conf. Ser. **161**, 012029 (2009).

[18] F. Beaudoin, J. M. Gambetta, and A. Blais, Dissipation and ultrastrong coupling in circuit QED, Phys. Rev. A **84**, 043832 (2011).

[19] S. de Liberato, D. Gerace, I. Carusotto, and C. Ciuti, Extracavity quantum vacuum radiation from a single qubit, Phys. Rev. A **80**, 053810 (2009).

[20] I. Carusotto, S. De Liberato, D. Gerace, and C. Ciuti, Back-reaction effects of quantum vacuum in cavity quantum electrodynamics, Phys. Rev. A **85**, 023805 (2012).

[21] L. Garziano, A. Ridolfo, R. Stassi, O. Di Stefano, and S. Savasta, Switching on and off of ultrastrong light-matter interaction: Photon statistics of quantum vacuum radiation, Phys. Rev. A **88**, 063829 (2013).

[22] D. S. Shapiro, A. A. Zhukov, W. V. Pogosov, and Y. E. Lozovik, Dynamical Lamb effect in a tunable superconducting qubit-cavity system, Phys. Rev. A **91**, 063814 (2015).

[23] G. Günter, A. A. Anappara, J. Hees, A. Sell, G. Biasiol, L. Sorba, S. De Liberato, C. Ciuti, A. Tredicucci, A. Leitenstorfer, and R. Huber, Sub-cycle switch-on of ultrastrong ligh–matter interaction, Nature (London) **458**, 178 (2009).

[24] A. Ridolfo, R. Vilardi, O. Di Stefano, S. Portolan, and S. Savasta, All optical switch of vacuum Rabi oscillations: The ultrafast quantum eraser, Phys. Rev. Lett. **106**, 013601 (2011).

[25] J.-F. Huang and C. K. Law, Photon emission via vacuum-dressed intermediate states under ultrastrong coupling, Phys. Rev. A **89**, 033827 (2014).

[26] M. Cirio, S. De Liberato, N. Lambert, and F. Nori, Ground state electroluminescence, Phys. Rev. Lett. **116**, 113601 (2016).

[27] F. Minganti, A. Mercurio, F. Mauceri, M. Scigliuzzo, S. Savasta, and V. Savona, Phonon pumping by modulating the ultrastrong vacuum, SciPost Phys. **17**, 027 (2024).

[28] A. Mercurio, S. D. Liberato, F. Nori, S. Savasta, and R. Stassi, Flying atom back-reaction and mechanically generated photons from vacuum, arXiv:2209.10419.

[29] V. Macrì, A. Ridolfo, O. Di Stefano, A. F. Kockum, F. Nori, and S. Savasta, Nonperturbative dynamical Casimir effect in optomechanical systems: Vacuum casimir-Rabi splittings, Phys. Rev. X **8**, 011031 (2018).

[30] J. R. Johansson, G. Johansson, C. M. Wilson, and F. Nori, Dynamical Casimir effect in a superconducting Coplanar waveguide, Phys. Rev. Lett. **103**, 147003 (2009).

[31] J. R. Johansson, G. Johansson, C. M. Wilson, and F. Nori, Dynamical Casimir effect in superconducting microwave circuits, Phys. Rev. A **82**, 052509 (2010).

[32] J. R. Johansson, G. Johansson, C. M. Wilson, P. Delsing, and F. Nori, Nonclassical microwave radiation from the dynamical Casimir effect, Phys. Rev. A **87**, 043804 (2013).

[33] C. M. Wilson, G. Johansson, A. Pourkabirian, M. Simoen, J. R. Johansson, T. Duty, F. Nori, and P. Delsing, Observation of the dynamical Casimir effect in a superconducting circuit, Nature (London) **479**, 376 (2011).

[34] D. A. R. Dalvit, Shaking photons out of the vacuum, Nature (London) **479**, 303 (2011).

[35] O. Di Stefano, A. Settineri, V. Macrì, A. Ridolfo, R. Stassi, A. F. Kockum, S. Savasta, and F. Nori, Interaction of mechanical oscillators mediated by the exchange of virtual photon pairs, Phys. Rev. Lett. **122**, 030402 (2019).

[36] A. Settineri, V. Macrì, L. Garziano, O. Di Stefano, F. Nori, and S. Savasta, Conversion of mechanical noise into correlated photon pairs: Dynamical Casimir effect from an incoherent mechanical drive, Phys. Rev. A **100**, 022501 (2019).

[37] W. Qin, V. Macrì, A. Miranowicz, S. Savasta, and F. Nori, Emission of photon pairs by mechanical stimulation of the squeezed vacuum, Phys. Rev. A **100**, 062501 (2019).

[38] D. De Bernardis, P. Pilar, T. Jaako, S. De Liberato, and P. Rabl, Breakdown of gauge invariance in ultrastrong-coupling cavity QED, Phys. Rev. A **98**, 053819 (2018).

[39] W. Salmon, C. Gustin, A. Settineri, O. D. Stefano, D. Zueco, S. Savasta, F. Nori, and S. Hughes, Gauge-independent emission spectra and quantum correlations in the ultrastrong coupling regime of open system cavity-QED, Nanophotonics **11**, 1573 (2022).

[40] K. Akbari, W. Salmon, F. Nori, and S. Hughes, Generalized Dicke model and gauge-invariant master equations for two atoms in ultrastrongly-coupled cavity quantum electrodynamics, Phys. Rev. Res. **5**, 033002 (2023).

[41] A. Settineri, V. Macrì, A. Ridolfo, O. Di Stefano, A. F. Kockum, F. Nori, and S. Savasta, Dissipation and thermal noise in hybrid quantum systems in the ultrastrong-coupling regime, Phys. Rev. A **98**, 053834 (2018).

[42] V. Macrì, A. Mercurio, F. Nori, S. Savasta, and C. Sánchez Muñoz, Spontaneous scattering of Raman photons from cavity-QED systems in the ultrastrong coupling regime, Phys. Rev. Lett. **129**, 273602 (2022).

[43] G. Floquet, Sur les équations différentielles linéaires à coefficients périodiques, Ann. Sci. l'École Norm. Supér. **12**, 47 (1883).

[44] M. Grifoni and P. Hänggi, Driven quantum tunneling, Phys. Rep. **304**, 229 (1998).

[45] T. Iadecola and C. Chamon, Floquet systems coupled to particle reservoirs, Phys. Rev. B **91**, 184301 (2015).

[46] T. Oka and S. Kitamura, Floquet engineering of quantum materials, Annu. Rev. Condens. Matter Phys. **10**, 387 (2019).

[47] O. R. Diermann and M. Holthaus, Floquet-state cooling, Sci. Rep. **9**, 17614 (2019).

[48] C. Weitenberg and J. Simonet, Tailoring quantum gases by Floquet engineering, Nat. Phys. **17**, 1342 (2021).

[49] J. N. Bandyopadhyay and J. Thingna, Floquet engineering of Lie algebraic quantum systems, Phys. Rev. B **105**, L020301 (2022).

[50] F. Petiziol and A. Eckardt, Cavity-based reservoir engineering for Floquet-engineered superconducting circuits, Phys. Rev. Lett. **129**, 233601 (2022).

[51] H. Liu, H. Cao, and S. Meng, Floquet engineering of topological states in realistic quantum materials via light-matter interactions, Prog. Surf. Sci. **98**, 100705 (2023).

[52] A. Castro, U. D. Giovannini, S. A. Sato, H. Hübener, and A. Rubio, Floquet engineering with quantum optimal control theory, New J. Phys. **25**, 043023 (2023).

[53] F. Zhan, J. Zeng, Z. Chen, X. Jin, J. Fan, T. Chen, and R. Wang, Floquet engineering of nonequilibrium valley-polarized quantum anomalous Hall effect with tunable Chern number, Nano Lett. **23**, 2166 (2023).

[54] S. Geier, N. Thaicharoen, C. Hainaut, T. Franz, A. Salzinger, A. Tebben, D. Grimshandl, G. Zürn, and M. Weidemüller, Floquet Hamiltonian engineering of an isolated many-body spin system, Science **374**, 1149 (2021).

[55] S.-Y. Bai and J.-H. An, Floquet engineering to overcome no-go theorem of noisy quantum metrology, Phys. Rev. Lett. **131**, 050801 (2023).

[56] A. Schnell, C. Weitenberg, and A. Eckardt, Dissipative preparation of a Floquet topological insulator in an optical lattice via bath engineering, SciPost Phys. **17**, 052 (2024).

[57] U. Kumar, S. Banerjee, and S.-Z. Lin, Floquet engineering of Kitaev quantum magnets, Commun. Phys. **5**, 1 (2022).

[58] P. K. Tien and J. P. Gordon, Multiphoton process observed in the interaction of microwave fields with the tunneling between superconductor films, Phys. Rev. **129**, 647 (1963).

[59] F. Grossmann, T. Dittrich, P. Jung, and P. Hänggi, Coherent destruction of tunneling, Phys. Rev. Lett. **67**, 516 (1991).

[60] G. Platero and R. Aguado, Photon-assisted transport in semiconductor nanostructures, Phys. Rep. **395**, 1 (2004).

[61] A. Eckardt, T. Jinasundera, C. Weiss, and M. Holthaus, Analog of photon-assisted tunneling in a Bose-Einstein condensate, Phys. Rev. Lett. **95**, 200401 (2005).

[62] K. Shibata, A. Umeno, K. M. Cha, and K. Hirakawa, Photon-assisted tunneling through self-assembled InAs quantum dots in the terahertz frequency range, Phys. Rev. Lett. **109**, 077401 (2012).

[63] W. A. Coish and J. M. Gambetta, Entangled photons on demand: Erasing which-path information with sidebands, Phys. Rev. B **80**, 241303(R) (2009).

[64] L. Yuan and S. Fan, Topologically nontrivial Floquet band structure in a system undergoing photonic transitions in the ultrastrong-coupling regime, Phys. Rev. A **92**, 053822 (2015).

[65] J. Xu, C. Zhong, X. Han, D. Jin, L. Jiang, and X. Zhang, Floquet cavity electromagnonics, Phys. Rev. Lett. **125**, 237201 (2020).

[66] S. Hughes, Breakdown of the area theorem: Carrier-wave Rabi flopping of femtosecond optical pulses, Phys. Rev. Lett. **81**, 3363 (1998).

[67] M. F. Ciappina, J. A. Pérez-Hernández, A. S. Landsman, T. Zimmermann, M. Lewenstein, L. Roso, and F. Krausz, Carrier-wave Rabi-flopping signatures in high-order harmonic generation for alkali atoms, Phys. Rev. Lett. **114**, 143902 (2015).

[68] O. D. Mücke, T. Tritschler, M. Wegener, U. Morgner, and F. X. Kärtner, Signatures of carrier-wave Rabi flopping in GaAs, Phys. Rev. Lett. **87**, 057401 (2001).

[69] O. Di Stefano, A. Settineri, V. Macrì, L. Garziano, R. Stassi, S. Savasta, and F. Nori, Resolution of gauge ambiguities in ultrastrong-coupling cavity quantum electrodynamics, Nat. Phys. **15**, 803 (2019).

[70] M. A. D. Taylor, A. Mandal, W. Zhou, and P. Huo, Resolution of gauge ambiguities in molecular cavity quantum electrodynamics, Phys. Rev. Lett. **125**, 123602 (2020).

[71] M. A. D. Taylor, A. Mandal, and P. Huo, Resolving ambiguities of the mode truncation in cavity quantum electrodynamics, Opt. Lett. **47**, 1446 (2022).

[72] A. Settineri, O. Di Stefano, D. Zueco, S. Hughes, S. Savasta, and F. Nori, Gauge freedom, quantum measurements, and time-dependent interactions in cavity QED, Phys. Rev. Res. **3**, 023079 (2021).

[73] C. Gustin, S. Franke, and S. Hughes, Gauge-invariant theory of truncated quantum light-matter interactions in arbitrary media, Phys. Rev. A **107**, 013722 (2023).

[74] P. Delsing *et al.*, The 2019 surface acoustic waves roadmap, J. Phys. D **52**, 353001 (2019).

[75] F. Iikawa, A. Hernández-Mínguez, M. Ramsteiner, and P. V. Santos, Optical phonon modulation in semiconductors by surface acoustic waves, Phys. Rev. B **93**, 195212 (2016).

[76] P. Roelli, C. Galland, N. Piro, and T. J. Kippenberg, Molecular cavity optomechanics as a theory of plasmon-enhanced Raman scattering, Nat. Nanotechnol. **11**, 164 (2015).

[77] M. K. Schmidt, R. Esteban, A. González-Tudela, G. Giedke, and J. Aizpurua, Quantum mechanical description of Raman scattering from molecules in plasmonic cavities, ACS Nano **10**, 6291 (2016).

[78] M. K. Dezfouli, R. Gordon, and S. Hughes, Molecular optomechanics in the anharmonic cavity-QED regime using hybrid metal–dielectric cavity modes, ACS Photonics **6**, 1400 (2019).

[79] M. Abramowitz and I. Stegun, *Handbook of Mathematical Functions: With Formulas, Graphs, and Mathematical Tables*, Applied Mathematics Series (Dover Publications, New York, 1965).

[80] S. Ashhab, J. R. Johansson, A. M. Zagoskin, and F. Nori, Two-level systems driven by large-amplitude fields, Phys. Rev. A **75**, 063414 (2007).

[81] A. I. Nikishov and V. I. Ritus, Quantum processes in the field of a plane electromagnetic wave and in a constant field 1, Sov. Phys. JETP **19**, 529 (1964).

[82] C. Chicone, *Ordinary Differential Equations with Applications*, Texts in Applied Mathematics (Springer, New York, 2006).

[83] J. H. Shirley, Solution of the Schrödinger equation with a Hamiltonian periodic in time, Phys. Rev. **138**, B979 (1965).

[84] See Supplemental Material at http://link.aps.org/supplemental/10.1103/PhysRevLett.134.063602, which also includes Refs. [85–93], for further details of the system Hamiltonian we use for the time-dependent quantum Rabi model, the general Floquet theory, additional results and discussions, further numerical simulations, and different modulation profiles for the time-dependent oscillations (specifically, different from the purely sinusoidal case shown in the main text).

[85] D. Braak, Integrability of the Rabi model, Phys. Rev. Lett. **107**, 100401 (2011).
[86] A. Eckardt and E. Anisimovas, High-frequency approximation for periodically driven quantum systems from a Floquet-space perspective, New J. Phys. **17**, 093039 (2015).
[87] H. Sambe, Steady states and quasienergies of a quantum-mechanical system in an oscillating field, Phys. Rev. A **7**, 2203 (1973).
[88] S. Restrepo, J. Cerrillo, P. Strasberg, and G. Schaller, From quantum heat engines to laser cooling: Floquet theory beyond the Born–Markov approximation, New J. Phys. **20**, 053063 (2018).
[89] S. Restrepo, Driven open quantum systems: Aspects of non-Markovianity and strong coupling, Ph.D. thesis, Technische Universität Berlin, 2019.
[90] M. D. Schroer, M. H. Kolodrubetz, W. F. Kindel, M. Sandberg, J. Gao, M. R. Vissers, D. P. Pappas, A. Polkovnikov, and K. W. Lehnert, Measuring a topological transition in an artificial spin-$1/2$ system, Phys. Rev. Lett. **113**, 050402 (2014).
[91] J. Hausinger, Dissipative dynamics of a qubit-oscillator system in the ultrastrong coupling and driving regimes, Ph.D. thesis, Universität Regensburg, 2010.
[92] S.-K. Son, S. Han, and Shih-I. Chu, Floquet formulation for the investigation of multiphoton quantum interference in a superconducting qubit driven by a strong ac field, Phys. Rev. A **79**, 032301 (2009).
[93] A. M. Satanin, M. V. Denisenko, S. Ashhab, and F. Nori, Amplitude spectroscopy of two coupled qubits, Phys. Rev. B **85**, 184524 (2012).
[94] S.-I. Chu, J. V. Tietz, and K. K. Datta, Quantum dynamics of molecular multiphoton excitation in intense laser and static electric fields: Floquet theory, quasienergy spectra, and application to the HF molecule, J. Chem. Phys. **77**, 2968 (1982).
[95] S.-I. Chu, *Recent Developments in Semiclassical Floquet Theories for Intense-Field Multiphoton Processes* (Academic Press, New York, 1985), pp. 197–253.
[96] S.-I. Chu and D. A. Telnov, Beyond the Floquet theorem: Generalized Floquet formalisms and quasienergy methods for atomic and molecular multiphoton processes in intense laser fields, Phys. Rep. **390**, 1 (2004).
[97] T.-S. Ho, K. Wang, and Shih-I. Chu, Floquet-Liouville supermatrix approach: Time development of density-matrix operator and multiphoton resonance fluorescence spectra in intense laser fields, Phys. Rev. A **33**, 1798 (1986).
[98] H. P. Breuer and M. Holthaus, Adiabatic processes in the ionization of highly excited hydrogen atoms, Z. Phys. D **11**, 1 (1989).
[99] H. Breuer and M. Holthaus, Quantum phases and Landau-Zener transitions in oscillating fields, Phys. Lett. A **140**, 507 (1989).
[100] M. Holthaus, Floquet engineering with quasienergy bands of periodically driven optical lattices, J. Phys. B **49**, 013001 (2015).
[101] S. Hughes, C. Gustin, and F. Nori, Reconciling quantum and classical spectral theories of ultrastrong coupling: Role of cavity bath coupling and gauge corrections, Opt. Quantum **2**, 133 (2024).
[102] A. Eckardt, Colloquium: Atomic quantum gases in periodically driven optical lattices, Rev. Mod. Phys. **89**, 011004 (2017).
[103] N. Vitanov, B. Shore, L. Yatsenko, K. Böhmer, T. Halfmann, T. Rickes, and K. Bergmann, Power broadening revisited: Theory and experiment, Opt. Commun. **199**, 117 (2001).
[104] S. H. Autler and C. H. Townes, Stark effect in rapidly varying fields, Phys. Rev. **100**, 703 (1955).
[105] C. N. Cohen-Tannoudji, The Autler-Townes effect revisited, in *Amazing Light: A Volume Dedicated To Charles Hard Townes On His 80th Birthday* (Springer, New York, 1996), pp. 109–123.
[106] E. H. Ahmed, J. Huennekens, T. Kirova, J. Qi, and A. M. Lyyra, The Autler–Townes effect in molecules: Observations, theory, and applications, in *Advances in Atomic, Molecular, and Optical Physics*, Advances in Atomic, Molecular, and Optical Physics Vol. 61, edited by P. Berman, E. Arimondo, and C. Lin (Academic Press, New York, 2012), pp. 467–514.
[107] B. Peng, S. K. Özdemir, W. Chen, F. Nori, and L. Yang, What is and what is not electromagnetically induced transparency in whispering-gallery microcavities, Nat. Commun. **5**, 5082 (2014).
[108] K. Ono, S. N. Shevchenko, T. Mori, S. Moriyama, and F. Nori, Quantum interferometry with a g-factor-tunable spin qubit, Phys. Rev. Lett. **122**, 207703 (2019).